PAPER

cRGD-installed docetaxel-loaded mertansine prodrug micelles: redox-triggered ratiometric dual drug release and targeted synergistic treatment of B16F10 melanoma

To cite this article: Ping Zhong *et al* 2017 *Nanotechnology* **28** 295103

View the article online for updates and enhancements.

Related content

- Phenylboronic acid-decorated gelatin nanoparticles for enhanced tumor targeting and penetration
Xin Wang, Bing Wei, Xu Cheng et al.
- Hyaluronic acid modified mesoporous carbon nanoparticles for targeted drug delivery to CD44-overexpressing cancer cells
Long Wan, Jian Jiao, Yu Cui et al.
- Combination chemotherapy of doxorubicin, all-trans retinoic acid and low molecular weight heparin based on self-assembled multi-functional polymeric nanoparticles
Ting Zhang, Hui Xiong, Fatima Zohra Dahmani et al.

Recent citations

- Cancer-targeted and glutathione-responsive micellar carriers for controlled delivery of cabazitaxel
Xiaoxiong Han *et al*
- Peptide-decorated polymeric nanomedicines for precision cancer therapy
Huanli Sun *et al*
- Redox-responsive nano-carriers as tumor-targeted drug delivery systems
Ali Raza *et al*

IOP ebooks™

Bringing you innovative digital publishing with leading voices to create your essential collection of books in STEM research.

Start exploring the collection - download the first chapter of every title for free.

This content was downloaded from IP address 42.244.24.113 on 24/12/2018 at 07:01

IOP Publishing Nanotechnology

Nanotechnology **28** (2017) 295103 (11pp) https://doi.org/10.1088/1361-6528/aa76cc

cRGD-installed docetaxel-loaded mertansine prodrug micelles: redox-triggered ratiometric dual drug release and targeted synergistic treatment of B16F10 melanoma

Ping Zhong, Min Qiu, Jian Zhang, Huanli Sun, Ru Cheng[1], Chao Deng, Fenghua Meng and Zhiyuan Zhong[1]

Biomedical Polymers Laboratory, and Jiangsu Key Laboratory of Advanced Functional Polymer Design and Application, College of Chemistry, Chemical Engineering and Materials Science, Soochow University, Suzhou, 215123, People's Republic of China

E-mail: rcheng@suda.edu.cn and zyzhong@suda.edu.cn

Received 28 April 2017, revised 28 May 2017
Accepted for publication 2 June 2017
Published 30 June 2017

Abstract

Combinatorial chemotherapy, which has emerged as a promising treatment modality for intractable cancers, is challenged by a lack of tumor-targeting, robust and ratiometric dual drug release systems. Here, docetaxel-loaded cRGD peptide-decorated redox-activable micellar mertansine prodrug (DTX-cRGD-MMP) was developed for targeted and synergistic treatment of B16F10 melanoma-bearing C57BL/6 mice. DTX-cRGD-MMP exhibited a small size of ca. 49 nm, high DTX and DM1 loading, low drug leakage under physiological conditions, with rapid release of both DTX and DM1 under a cytoplasmic reductive environment. Notably, MTT and flow cytometry assays showed that DTX-cRGD-MMP brought about a synergistic antitumor effect to B16F10 cancer cells, with a combination index of 0.37 and an IC_{50} over 3- and 13-fold lower than cRGD-MMP (w/o DTX) and DTX-cRGD-Ms (w/o DM1) controls, respectively. *In vivo* studies revealed that DTX-cRGD-MMP had a long circulation time and a markedly improved accumulation in the B16F10 tumor compared with the non-targeting DTX-MMP control (9.15 versus 3.13% ID/g at 12 h post-injection). Interestingly, mice treated with DTX-cRGD-MMP showed almost complete growth inhibition of B16F10 melanoma, with tumor inhibition efficacy following an order of DTX-cRGD-MMP > DTX-MMP (w/o cRGD) > cRGD-MMP (w/o DTX) > DTX-cRGD-Ms (w/o DM1) > free DTX. Consequently, DTX-cRGD-MMP significantly improved the survival rates of B16F10 melanoma-bearing mice. Importantly, DTX-cRGD-MMP caused little adverse effects as revealed by mice body weights and histological analyses. The combination of two mitotic inhibitors, DTX and DM1, appears to be an interesting approach for effective cancer therapy.

Supplementary material for this article is available online

Keywords: combinatorial chemotherapy, targeted delivery, mitotic inhibitor, reduction-sensitive, melanoma

(Some figures may appear in colour only in the online journal)

[1] Authors to whom any correspondence should be addressed.

 © 2017 IOP Publishing Ltd Printed in the UK

1. Introduction

Combinatorial chemotherapy with two or more drugs that inhibit the growth of cancer cells using different mechanisms is a successful approach to treat various cancers in the clinic [1, 2]. The combinatorial effect of dual or multiple chemotherapeutics might effectively slow cancer cell mutation, overcome drug resistance, and increase therapeutic outcomes [3]. In practice, however, combination chemotherapy is challenged by the varying water solubility, pharmacokinetic profiles and membrane transport properties of different anticancer drugs [4–6]. In addition, administration of two or more free drugs could possibly lead to higher toxic side effects [7]. Co-delivery of different drugs in a single nanocarrier system may afford a more effective and safer combination cancer therapy, as both drugs are simultaneously delivered to the tumor sites and off-site side effects are reduced [8–11]. The physical encapsulation of multiple drugs in a single nanocarrier is, nevertheless, associated with several challenges including low drug loading content and poor stability [12]. In past years, polymeric prodrugs have appeared as a versatile platform for combination cancer chemotherapy [13–18]. For example, Zhou *et al* reported that 10-hydroxycamptothecin (HCPT)-loaded doxorubicin (DOX) conjugated PEG-SS-PCL micelles exhibited a high therapeutic efficacy in the MCF-7/ADR tumor model and effectively prevented lung metastasis [17]. Haam *et al* reported that poly(L-lysine)-paclitaxel (PLL-PTX) and hyaluronic acid-gemcitabine (HA-GEM) conjugates showed a synergistic inhibition effect in HuCCT1 tumor xenografts [18].

Mertansine (DM1), a strong antiproliferative chemotherapeutics toward over 60 types of cancer cell lines, has received intensive interest in the development of antibody-maytansinoid conjugates (AMCs) for treating various malignancies such as breast cancer and melanoma [19–22]. DM1 is a powerful antimitotic agent that binds with strong affinity to tubulins, inhibits the tubulins polymerization and arrests cell mitosis [23–25]. However, the clinical application of DM1 is limited by its high systemic toxicity and small therapeutic window [26]. We recently found that cRGD-functionalized micellar mertansine prodrug (cRGD-MMP) based on poly(ethylene glycol)-*b*-(poly(trimethylene carbonate)-*graft*-SSDM1) (PEG-P(TMC-*g*-SSDM1)) and cRGD peptide functionalized PEG-P(TMC-*g*-SSDM1) had a high drug loading content, better drug toleration and significantly improved therapeutic effects in the B16F10 melanoma model as compared to free DM1 [27].

Here, we report that cRGD-MMP loading with docetaxel (DTX), a well-known mitotic inhibitor that blocks cell division by interfering with spindle formation during cell mitosis, for targeted combinatorial chemotherapy of malignant B16F10 melanoma-bearing C57BL/6 mice (Scheme 1). DTX has been used for the treatment of non-small cell lung cancer, prostate cancer and melanoma [28–30]. Given their different working mechanisms, co-administration of DM1 and DTX in a single nanocarrier system might result in a synergistic treatment effect with reduced side effects. cRGD peptide has shown a strong binding toward $\alpha_v\beta_3$ integrin-overexpressed B16F10 melanoma cells [31–34]. Notably, our results demonstrated easy loading of DTX into cRGD-MMP and redox-triggered ratiometric release of DTX and DM1. DTX-loaded cRGD-MMP (DTX-cRGD-MMP) exhibited synergistic growth inhibition of B16F10 cancer cells *in vitro* and treatment of B16F10 melanoma *in vivo*.

2. Materials and methods

2.1. Materials

N_2'-deacetyl-N_2'-(3-mercapto-1-oxopropyl)-maytansine (DM1, Suzhou Brightgene Co., Ltd), docetaxel (DTX, Beijing ZhongShuo Pharmaceutical Technology Development Co., Ltd), annexin V-FITC/propidium iodide (PI) apoptosis detection kit (MesGen Biotech), 3-(4,5-dimethylthiazol-2-yl)-2,5-diphenyltetrazolium bromide (MTT, Sigma) and 4′6-diamidino-2-phenylindole dihydrochloride (DAPI, Sigma) were used as received. PEG-P(TMC-*g*-SSDM1) and cRGD-PEG-P(TMC-*g*-SSDM1) were synthesized according to our previous report [27].

2.2. Preparation of DTX-cRGD-MMP and DTX-MMP

DTX-loaded cRGD-decorated polymeric micellar mertansine prodrug (DTX-cRGD-MMP) was prepared from PEG-P(TMC-*g*-SSDM1) and cRGD-PEG-P(TMC-*g*-SSDM1) copolymers (w/w, 80/20) at a DTX theoretical loading content (DLC) of 28.5 wt.% via a solvent exchange method. Typically, 0.2 ml of DMF solution (5 mg ml^{-1}) of PEG-P(TMC-*g*-SSDM1) and cRGD-PEG-P(TMC-*g*-SSDM1) mixture (w/w, 80/20) with 40 μl DTX solution (10 mg ml^{-1}) was added dropwise to 0.8 ml of PB buffer (10 mM, pH 7.4) and stirred for another 2 h, followed by extensive dialysis (Spectra/Pore, MWCO 7000) against PB for 12 h. DTX-loaded PEG-P(TMC-*co*-PDSC) micelles (DTX-Ms), DTX-loaded cRGD-decorated PEG-P(TMC-*co*-PDSC) micelles (DTX-cRGD-Ms), and DTX-loaded PEG-P(TMC-*g*-SSDM1) micellar mertansine prodrug (DTX-MMP) were prepared in the same manner as DTX-cRGD-MMP. The amounts of DM1 and DTX were quantified by HPLC. DLC of DTX and DM1 was calculated according to the following formula:

DLC (wt.%) = (weight of DTX or DM1/weight of drug-loaded micelle) × 100.

2.3. In vitro antitumor performance and synergistic analysis of DM1 and DTX combination

MTT assays were performed to study the *in vitro* antitumor effects of DTX-cRGD-MMP, DTX-MMP as well as free DM1 and DTX combination. Briefly, B16F10 cells were grown in 96-well plates at 3 × 10^3 cells per well overnight. The different drug formulations at concentrations of 0.005–1 μg DM1 equiv./ml or 0.005–1 μg DTX equiv./ml were added. After 4 h, the medium was replaced by 100 μl fresh medium. The cells were cultured for another 44 h. 20 μl of 3-(4,5-dimethylthiazol-2-yl)-2,5-diphenyltetrazolium bromide (MTT) solution (5 mg ml^{-1}) was added. The cells were

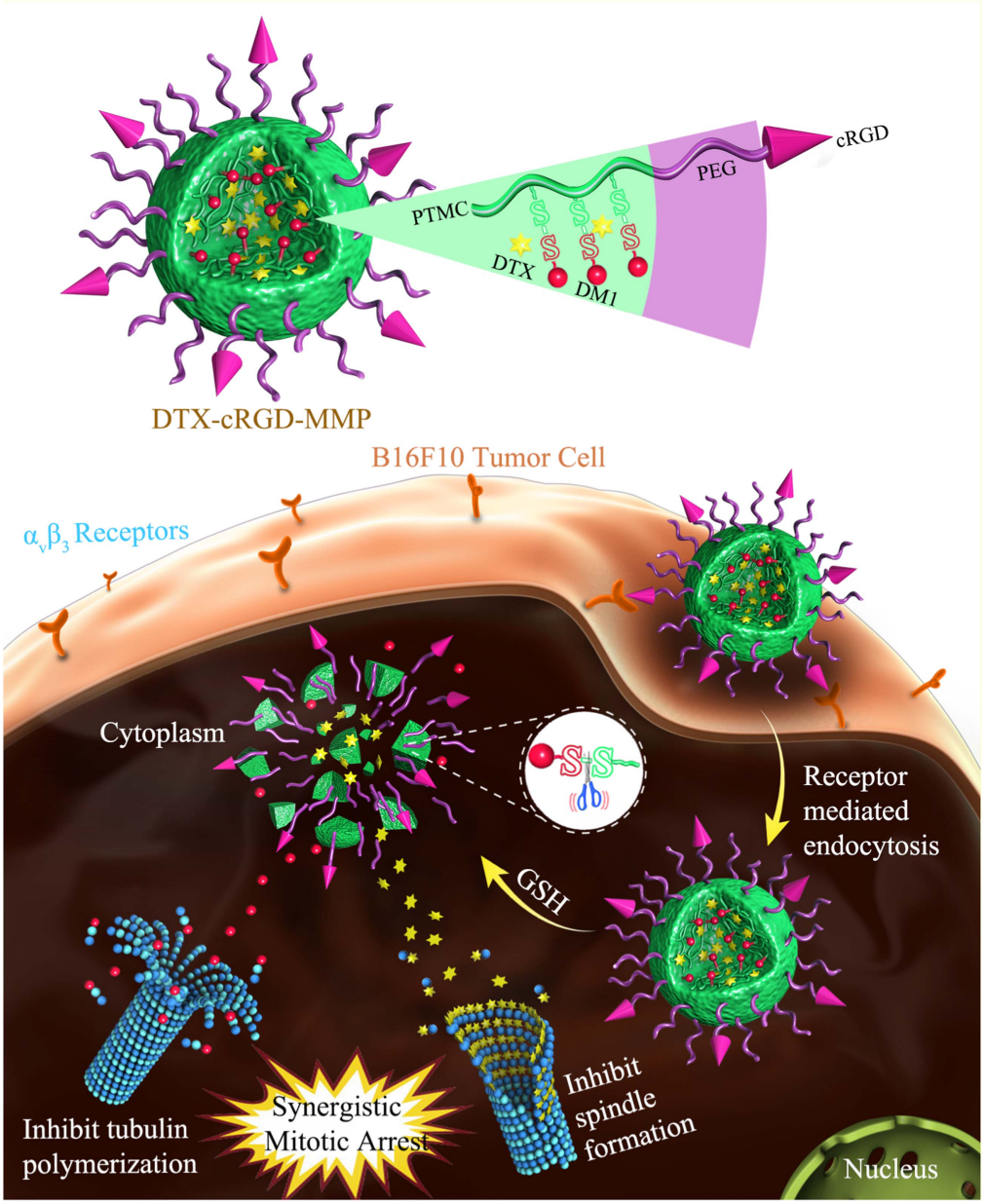

Scheme 1. DTX-cRGD-MMP for targeted and combinatorial treatment of B16F10 melanoma cells via synergistic mitotic arrest.

further cultured for 4 h, the medium was removed, and 150 μl DMSO was added to dissolve the MTT-formazan crystals. The absorbance of the above solution in each well was recorded using a microplate reader (Thermo Fisher, Multiscan FC USD4600) at 492 nm. The cell viability (%) was determined by comparing the absorbance at 492 nm with control wells containing only cell culture media. The results were presented as the average $\pm$ standard deviation ($n = 4$).

IC_{50} was determined from the dose response curve. Combination index (CI_{50}) values were calculated according to the following formula: $CI_{50} = D_1/D_{m1} + D_2/D_{m2}$, where D_{m1} and D_{m2} are the IC_{50} concentrations of each drug alone, and D_1 and D_2 are the IC_{50} concentrations of each drug in the combination. CI_{50} value of >1, $=1$ and <1 indicates antagonistic, additive, and synergistic effects, respectively. CI_{50} values ranging from 0.2–0.8 are considered validated [35].

2.4. Cell apoptosis assays

The cell apoptosis assay of DTX-cRGD-MMP was performed in B16F10 cells using annexin V−FITC/propidium iodide (PI) staining. In brief, B16F10 cells at 3×10^4 cells per well were seeded in a 12-well plate overnight. Free DTX, free DM1, DTX + DM1, DTX-cRGD-Ms, cRGD-MMP, DTX-cRGD-MMP or DTX-MMP was added (dosage: 0.1 μg DM1 equiv./ml or 0.06 μg DTX equiv./ml). Cells without treatment were used as a control. After 4 h, the medium was replaced and the cells were cultured in 1000 μl fresh medium for another 20 h. The cells were harvested and collected by centrifugation, washed with PB three times, re-suspended in binding buffer, and labeled with annexin V−FITC and a PI apoptosis detection kit according to the instructions of manufacturer. After incubation in the dark for 15 min, cells were

analyzed on a BD FACS Calibur flow cytometer (Beckton Dickinson, USA) using Cell Quest software.

2.5. In vivo pharmacokinetic studies of DTX-cRGD-MMP and DTX-MMP

The mice were all handled under the guidelines approved by the Soochow University Laboratory Animal Center and the Animal Care and Use Committee of Soochow University. The pharmacokinetic studies of DTX-cRGD-MMP and DTX-MMP were performed in normal C57BL/6 mice (dosage: 5 mg DM1 equiv./kg or 3 mg DTX equiv./kg). The blood samples were collected at 0.083, 0.5, 0.75, 1, 2, 4, 8, 12, or 24 h post-injection of DTX-cRGD-MMP or DTX-MMP. 0.2 ml of methanol was added, the mixture was ultrasonicated for 15 min, and 0.5 ml of DMSO was added to extract DTX and DM1 prodrug under shaking (200 rpm) at 37 °C for one day followed by centrifugation (18 krpm, 20 min). To the supernatant was added excess DTT (50 mM) to completely release DM1 and DTX. The amounts of DM1 or DTX were quantified by HPLC. The results were presented as the average ± standard deviation ($n = 4$). The elimination half-life ($t_{1/2,\beta}$) was determined by fitting the experimental data using the Origin 8 exponential decay 2 model: $y = A_1 \times \exp(-x/t_1) + A_2 \times \exp(-x/t_2) + y_0$ and taking $t_{1/2,\beta} = 0.693\ t_2$.

2.6. In vivo combination therapy of melanoma

The *in vivo* antitumor efficacy and safety of DTX-cRGD-MMP and DTX-MMP were evaluated in B16F10 melanoma-bearing mice. 6×10^6 B16F10 cells in 50 μl of PBS were subcutaneously injected in the hind flank of C57BL/6 mice. When the tumor sizes reached around 30–50 mm^3 after 5 days implantation, the mice were weighted and randomly divided into six groups (n = 8) and this day was designed as day 0. The mice were intravenously administrated with PBS, free DTX, DTX-cRGD-Ms, cRGD-MMP, DTX-MMP or DTX-cRGD-MMP (dosage: 1.2 mg DM1 equiv./kg or 0.7 mg DTX equiv./kg). The mice were treated every two days for a total of three injections. Tumor sizes were recorded using calipers and calculated based on the following formula: $V = 0.5 \times L \times W^2$, where L and W are the tumor length and width, respectively [36]. The relative tumor volumes were ratios of tumor sizes at different time points to that at day 0. The body weights of all mice were weighed every two days throughout the entire treatment period. At day 10, three mice of each group were sacrificed and tumors were harvested, weighed and photographed. The remaining five mice of each group were used to monitor the survival rates. Tumor inhibition rate (TIR) was calculated according to the following formula: (1- (mean tumor weight of drug treated group/mean tumor weight of saline treated group)) × 100.

Table 1. Characteristics of DTX-cRGD-MMP and DTX-MMP.

			DLC (wt.%)[b]	
Formulations	Size[a] (d. nm)	PDI[a]	DM1	DTX
DTX-cRGD-MMP	49	0.12	21.7	12.5
DTX-MMP	45	0.10	21.7	13

[a] determined by DLS.
[b] determined by HPLC.

3. Results and discussion

3.1. Preparation and redox-triggered drug release of DTX-cRGD-MMP

PEG-P(TMC-*g*-SSDM1) and cRGD-PEG-P(TMC-*g*-SSDM1) were synthesized as reported previously [27]. As shown in table S1, available at stacks.iop.org/NANO/28/295103/mmedia, PEG-P(TMC-*co*-PDSC) was obtained with a moderate M_w/M_n of 1.6 and TMC and PDSC degree of polymerization (DP) of 40 and 4.5, respectively. The thiol-disulfide exchange between PEG-P(TMC-*co*-PDSC) and DM1 yielded PEG-P(TMC-*g*-SSDM1) with a DM1 content of 24.9 wt.%. Mal-PEG-P(TMC-*co*-PDSC) was prepared with a moderate M_w/M_n of 1.5 and TMC and PDSC DP of 40 and 4.8, respectively (table S1). The Michael-type conjugation of Mal-PEG-P(TMC-*co*-PDSC) with cyclo(RGD*f*C) peptide followed by thiol-disulfide exchange with DM1 furnished cRGD-PEG-P(TMC-*g*-SSDM1) with a quantitative cRGD functionality and DM1 content of 24.4 wt.%.

DTX-loaded cRGD-MMP was readily prepared from PEG-P(TMC-*g*-SSDM1) and cRGD-PEG-P(TMC-*g*-SSDM1) copolymers (w/w, 80/20) via a solvent exchange method. Notably, HPLC revealed a decent DTX loading content of 12.5 wt.% (table 1), likely due to the existence of strong interactions between DTX and DM1. In comparison, a DTX loading content of less than 10 wt.% was generally reported for micellar systems [37–39]. DLS showed that DTX-cRGD-MMP had a small size of 49 nm with a narrow PDI of 0.12 (figure 1(A)), which was further confirmed by a TEM image (figure 1(B)). The non-targeting DTX-MMP was obtained with a similar size (~45 nm) and DTX loading content (13 wt.%) to DTX-cRGD-MMP (table 1). In addition, we have also prepared DTX-loaded PEG-P(TMC-*co*-PDSC) micelles (DTX-Ms, w/o DM1 and targeting), DTX-loaded cRGD-decorated PEG-P(TMC-*co*-PDSC) micelles (DTX-cRGD-Ms, w/o DM1), cRGD-MMP (w/o DTX) and MMP (w/o DTX and targeting) as controls. DTX-Ms and DTX-cRGD-Ms had a size of ca. 60 nm and DTX loading content of ca. 12.5 wt.% (table S2). cRGD-MMP and MMP had a mean size of ca. 40 nm.

The *in vitro* release studies exhibited fast release of DM1 from DTX-cRGD-MMP in the presence of 10 mM GSH, in which over 50% and 80% of DM1 was released in 6 and 24 h, respectively (figure 2). In contrast, less than 15% DM1 was released in 24 h under a non-reductive condition. Interestingly, almost the same release profile was observed for DTX. This GSH-triggered DM1 and DTX release from DTX-

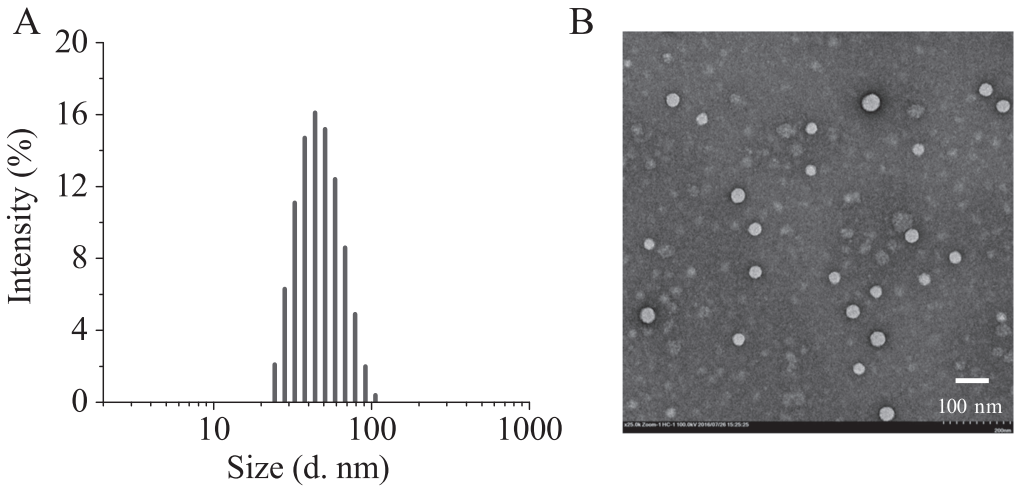

Figure 1. Size distribution of DTX-cRGD-MMP determined by DLS (a) and TEM (b).

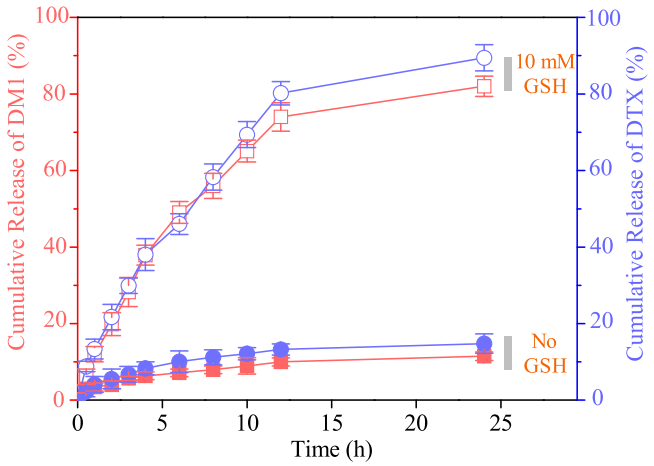

Figure 2. Cumulative release of DM1 and DTX from DTX-cRGD-MMP in PB buffer (pH 7.4, 10 mM) at a micelle concentration of 0.8 mg ml^{-1}, either with or without 10 mM GSH. The results are presented as mean ± standard deviation (n = 3).

cRGD-MMP is due to cleavage of disulfide bonds linking DM1 to polycarbonate, similar to hyaluronic acid-SS-DM1 prodrug [40] and others [41–43]. Figure S1 shows that non-targeting DTX-MMP had a similar DM1 and DTX release profile to DTX-cRGD-MMP, suggesting that cRGD peptide decoration does not affect their drug release behaviors. These results demonstrate that both DTX-cRGD-MMP and DTX-MMP are stable with little drug leakage under physiological condition while quickly and simultaneously releasing DM1 and DTX under a reductive condition, ensuring that the released DTX and DM1 maintain approximately the same drug ratio over time. It has been a great challenge to achieve ratiometric delivery and release of the two drugs [44, 45], which is, nevertheless, important for most combination therapy [46–49]. Huang *et al* achieved precise ratiometric release of gemcitabine and cisplatin over 96 h from poly(lactide-*co*-glycolide) (PLGA) nanoparticles that demonstrated enhanced treatment of a stroma-rich bladder tumor [46].

Table 2. IC_{50} and CI_{50} of DTX and DM1 in different formulations against B16F10 cells.

Formulations	IC_{50} (μg ml^{-1})		CI_{50}
	DTX	DM1	
DTX	0.39	—	—
DM1	—	0.092	—
DTX+DM1	0.047	0.079	0.98
DTX-Ms	0.78	—	—
MMP	—	0.43	—
DTX-MMP	0.049	0.081	0.25
DTX-cRGD-Ms	0.37	—	—
cRGD-MMP	—	0.16	—
DTX-cRGD-MMP	0.028	0.047	0.37

3.2. Synergistic antitumor effect of DTX-cRGD-MMP in vitro

The *in vitro* synergistic antitumor effect of DTX and DM1 in different formulations was investigated using MTT assays in malignant B16F10 melanoma cells. Figure S2 shows that blank micelles (i.e. Ms and cRGD-Ms) without any drug had little cytotoxicity. All drug formulations exhibited a dose-dependent cytotoxicity (figure S3). Notably, DTX-cRGD-MMP displayed significantly enhanced antitumor activities, in which DTX-cRGD-MMP had over 3- and 13-fold lower IC_{50} than cRGD-MMP and DTX-cRGD-Ms controls, respectively (table 2 and figure 3(a)). The CI was calculated, according to Chou-Talalay method [50], to be 0.37 and 0.25 for DTX-cRGD-MMP and DTX-MMP, respectively (figure S3(c)), confirming the strong synergistic antitumor effect of DTX and DM1. It is likely that the reduction triggered fast and ratiometric release of DTX and DM1 and significantly improves the synergistic killing effect. In recent years, microtubule-inhibiting agents including DTX and PTX have been combined with various chemotherapeutics such as DOX and Pt for enhanced growth inhibition of different cancer cells [51–54]. For instance, Chen *et al* reported that co-delivery of DOX and PTX resulted in a synergistic effect toward A549 human lung cancer cells with a CI_{50} of 0.57 [53]. Farokhzad

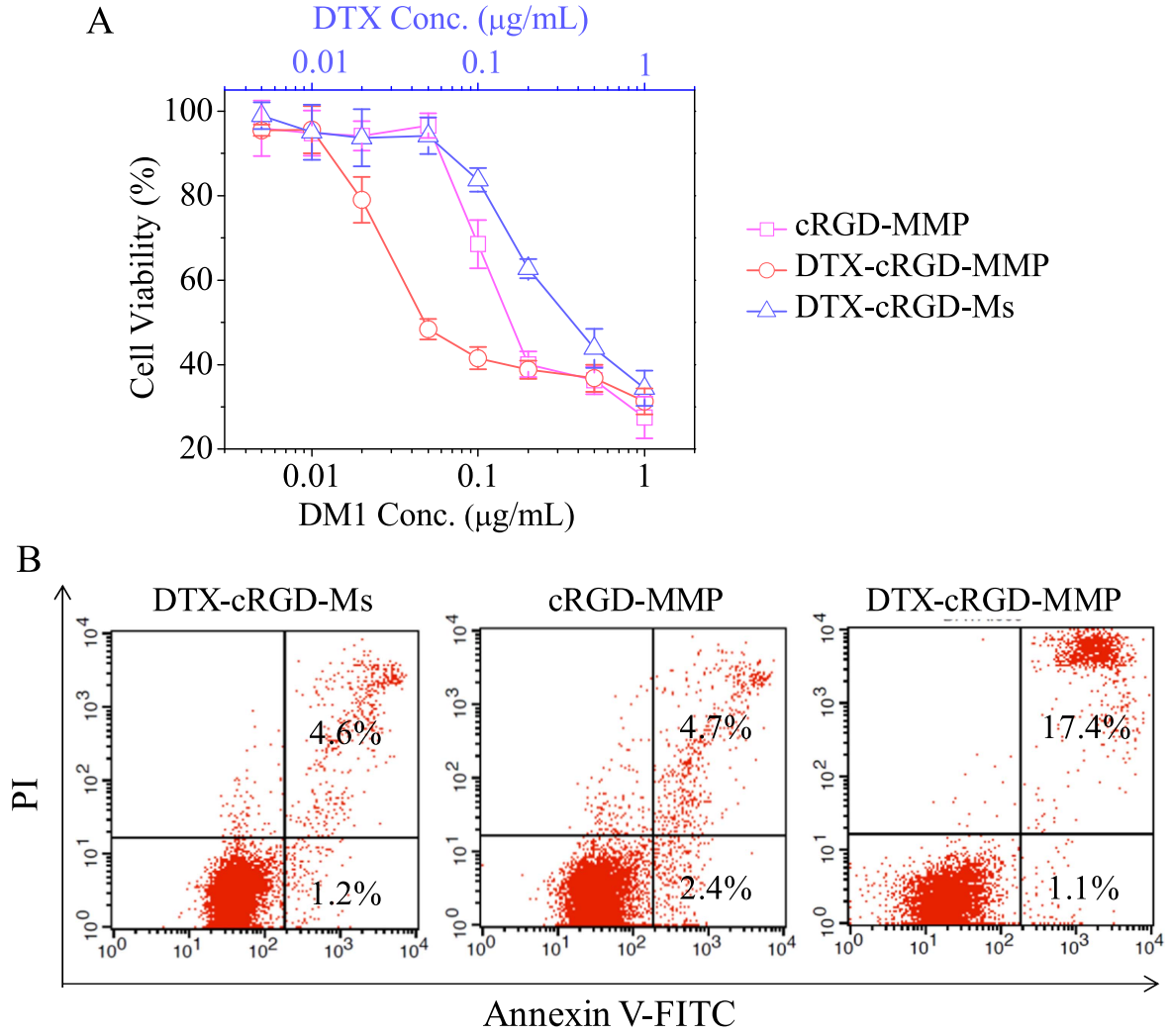

Figure 3. Synergistic antitumor effect of DTX-cRGD-MMP in B16F10 melanoma cells by MTT assays ($n = 4$) (a) and flow cytometry analysis (dosage: 0.1 μg DM1 equiv./ml, 0.06 μg DTX equiv./ml) (b).

et al reported that A10-aptamer-decorated DTX-loaded polymeric Pt-prodrug nanoparticles showed several times higher IC_{50} in LNCaP prostate cells than their respective single drug counterparts [55]. The results here showed that co-delivery of DTX and DM1, both of which inhibit tumor cell growth by inhibiting mitosis, is an effective strategy to achieve a combinatorial anticancer effect. It should be noted that no synergistic effect was observed for free DM1 and DTX (figure S3(a)), probably resulting from rapid internalization and dominant role of free DM1. Both DTX-cRGD-Ms and cRGD-MMP exhibited lower IC_{50} than the corresponding non-targeting controls (table 2), supporting that cRGD peptide decoration enhances the *in vitro* antitumor activity. It should be noted that as an initial proof-of-concept study on the combinatorial anticancer effect of DTX and DM1, here we have not optimized the drug ratio.

To further confirm the synergistic antitumor effect of DTX-cRGD-MMP, B16F10 cancer cells following annexin V-FITC/PI staining were quantitatively studied by flow cytometry. Figure 3(b) shows that DTX-cRGD-Ms (w/o MMP) and cRGD-MMP (w/o DTX) resulted in 5.8% and 7.1% apoptotic cells, respectively, which was much lower than 18.5% observed for DTX-cRGD-MMP. It should be noted that non-targeting DTX-MMP also induced 11.4% apoptosis (figure S4). In comparison, in line with the MTT results, no synergistic effect was discerned for free DM1 and DTX (figure S4). It is clear that DTX-cRGD-MMP possesses a strong synergistic antitumor effect in B16F10 melanoma cells.

3.3. In vivo pharmacokinetics and biodistribution of DTX-cRGD-MMP

In order to study their *in vivo* pharmacokinetics, DTX-cRGD-MMP and DTX-MMP were intravenously injected into C57BL/6 mice at 5 mg DM1 equiv./kg. DM1 and DTX levels in blood at designated time intervals were quantified by HPLC measurements. Considering that free DM1 has a low maximum-tolerated dose (MTD) of 1 mg kg^{-1}, which renders HPLC determination of blood DM1 concentration difficult, pharmacokinetic studies of free DM1 and DTX were not attempted. The pharmacokinetics of DM1 followed a typical two-compartment model (figure 4(a)). Interestingly, both

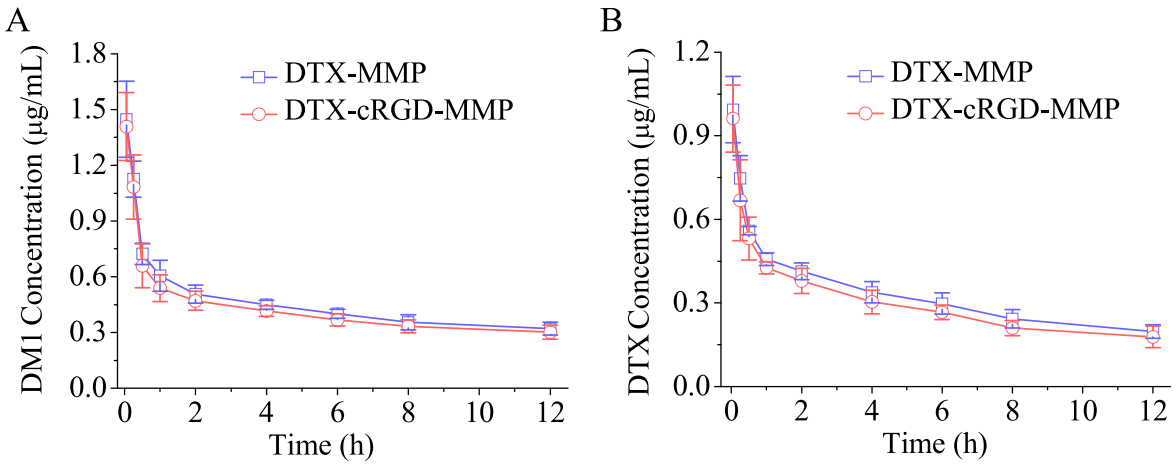

Figure 4. Pharmacokinetics of DTX-cRGD-MMP and DTX-MMP in C57BL/6 mice (5 mg DM1 equiv./kg, $n = 4$). (a) DM1, (b) DTX.

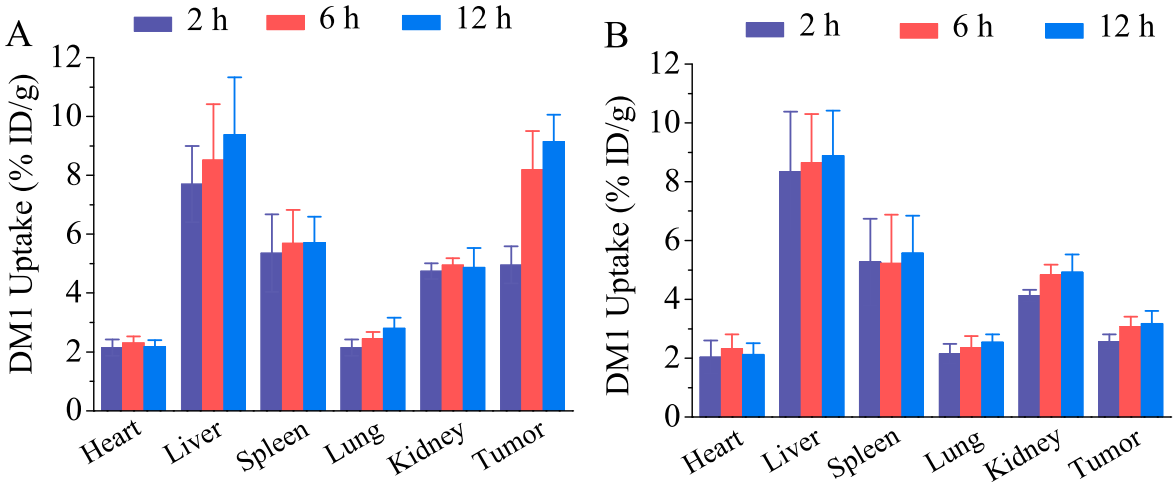

Figure 5. *In vivo* biodistribution of DTX-cRGD-MMP (a) and DTX-MMP (b) in B16F10 tumor bearing C57BL/6 mice following 2, 6 and 12 h intravenous injection (5 mg DM1 equiv./kg, $n = 4$).

DTX-cRGD-MMP and DTX-MMP had a long circulation time with an elimination half-life ($t_{1/2,\beta}$) of 4.03 and 4.50 h, respectively (table S3). The area under the curve (AUC) was 2.26 and 2.79 $\mu g \cdot h/ml$ for DTX-cRGD-MMP and DTX-MMP, respectively. Notably, DTX in both DTX-cRGD-MMP and DTX-MMP exhibited similar pharmacokinetic behaviors to DM1 (figure 4(b)), indicating little DTX leakage though DTX was physically encapsulated. The similar pharmacokinetics of DTX and DM1 warrants a steady DM1 and DTX ratio in DTX-cRGD-MMP during the blood circulation. In addition, little difference in drug clearance was observed for DTX-cRGD-MMP and DTX-MMP, suggesting that cRGD decoration hardly alters the pharmacokinetics.

The *in vivo* biodistribution of DTX-cRGD-MMP and DTX-MMP was evaluated in B16F10 melanoma-bearing C57BL/6 mice. The mice were sacrificed at 2, 6 or 12 h post-injection of DTX-cRGD-MMP or DTX-MMP (5 mg DM1 equiv./kg). As shown in figure 5(a), DTX-cRGD-MMP rapidly accumulated in the tumor, reaching 4.95% ID/g at 2 h post-injection, and increasing to 8.18% ID/g at 6 h. The amount of DM1 in the tumor reached 9.15% ID/g at 12 h post-injection. In comparison, much lower tumor accumulation of DM1 was observed for the non-targeting DTX-MMP, in which DM1 level maintained at about 3% ID/g at 2, 6 or 12 h post-injection (figure 5(b)). It should further be noted that DTX-cRGD-MMP has similar accumulation in the major organs to DTX-MMP. The plot of tumor-to-normal tissue (T/N) distribution ratios displayed that DTX-cRGD-MMP led to a 2–3 fold better tumor accumulation than DTX-MMP (figure S5). The enhanced tumor accumulation of DTX-cRGD-MMP likely results from the specific affinity of cRGD peptide to the $\alpha_v\beta_3$ integrins that are overexpressed on tumor neovasculatures as well as B16F10 melanoma cells [32, 56].

3.4. Combinatorial chemotherapy of B16F10 melanoma-bearing C57BL/6 mice

The *in vivo* therapeutic performances of DTX-cRGD-MMP and non-targeting DTX-MMP were studied in B16F10 melanoma-bearing C57BL/6 mice at 1.2 mg DM1 equiv./kg and 0.7 mg DTX equiv./kg for a total of three injections. Mice treated with PBS, free DTX, DTX-cRGD-Ms, and cRGD-MMP was applied as controls. As expected, PBS group

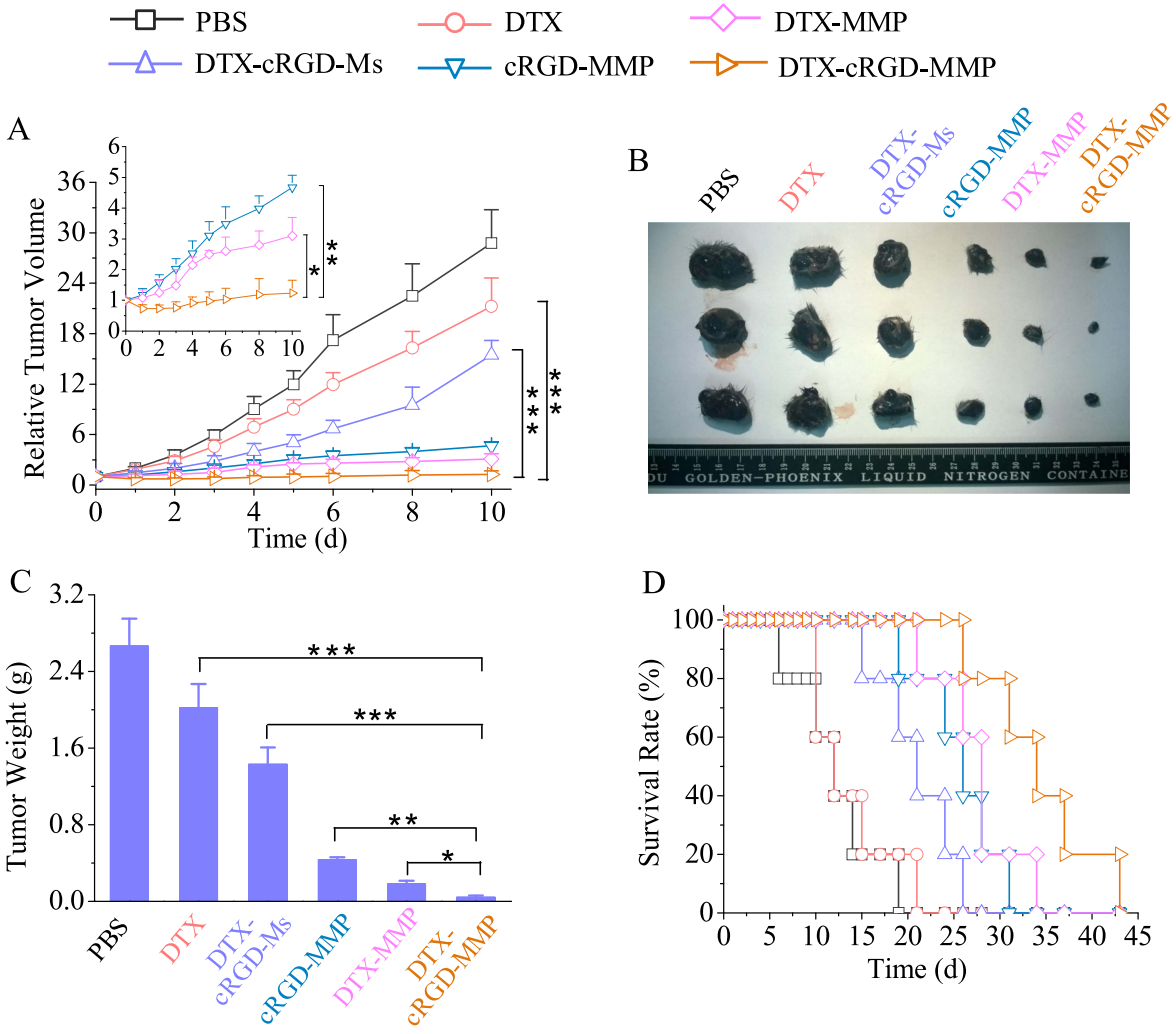

Figure 6. Synergistic treatment of B16F10 melanoma-bearing C57BL/6 mice with DTX-MMP and DTX-cRGD-MMP. Free DTX, DTX-cRGD-Ms and cRGD-MMP were used as controls. The drug was given on day 0, 2 and 4 for a total of three injections (dosages: 1.2 mg DM1 equiv./kg, 0.7 mg DTX equiv./kg). (a) Relative tumor volume ($n = 8$). $^{*}p < 0.05$, $^{**}p < 0.01$, $^{***}p < 0.001$ (Students' t test). Photographs (b) and weight (c) of typical tumor blocks collected from different treatment groups on day 10 ($n = 3$). (d) Survival rates of mice in different treatment groups.

displayed rapid tumor growth (figure 6(a)). The free DTX group showed modest tumor growth inhibition. DTX-cRGD-Ms demonstrated somewhat better tumor suppression than free DTX. Considering that free DM1 has a low MTD of 1 mg kg^{-1}, treatment with free DM1 was not attempted. Notably, DTX-cRGD-MMP exhibited almost complete tumor growth inhibition, which was obviously better than the cRGD-MMP control. Moreover, DTX-MMP also revealed effective inhibition of tumor growth, though to a lesser extent than DTX-cRGD-MMP. The tumor inhibition efficacy follows an order of DTX-cRGD-MMP > DTX-MMP > cRGD-MMP > DTX-cRGD-Ms > free DTX. On day 10, three mice in each group were sacrificed and tumors were collected, weighed and photographed. The remaining five mice of each group were used to monitor survival rates. The images of tumors showed clearly that mice treated with DTX-cRGD-MMP had the smallest size (figure 6(b)), supporting that DTX-cRGD-MMP has the best tumor growth inhibition. The co-delivery of rapamycin and cisplatin using anisamide-functionalized PLGA nanoparticles was reported to greatly enhance treatment of A375-luc melanoma-bearing mice though continued tumor growth was observed [57]. The DTX-cRGD-MMP group exhibited a superior tumor inhibition rate (TIR) of 98.2%, which was significantly higher than that of DTX-cRGD-Ms (TIR: 42.4%) and cRGD-MMP (TIR: 84.5%) (figure 6(c)). Notably, DTX-MMP also exhibited a great TIR of 92.7%. In comparison, co-delivery of DTX and tanespimycin using HA-decorated PLGA nanoparticles produced a moderate TIR of 75%, which was significantly higher than corresponding single drug formulations, in CD44 and RHAMM-overexpressing SCC-7 squamous cell carcinoma xenografts in nude mice [58]. The comparatively low TIR observed for dual drug-loaded PLGA nanoformulations with regard to DTX-cRGD-MMP is likely a result of slow drug release. Our previous report revealed that cRGD-MMP at a doubled DM1 dose (2.4 mg DM1 equiv./kg) caused a somewhat lower TIR in B16F10 melanoma than DTX-cRGD-MMP [27], supporting synergistic tumor inhibition of DM1

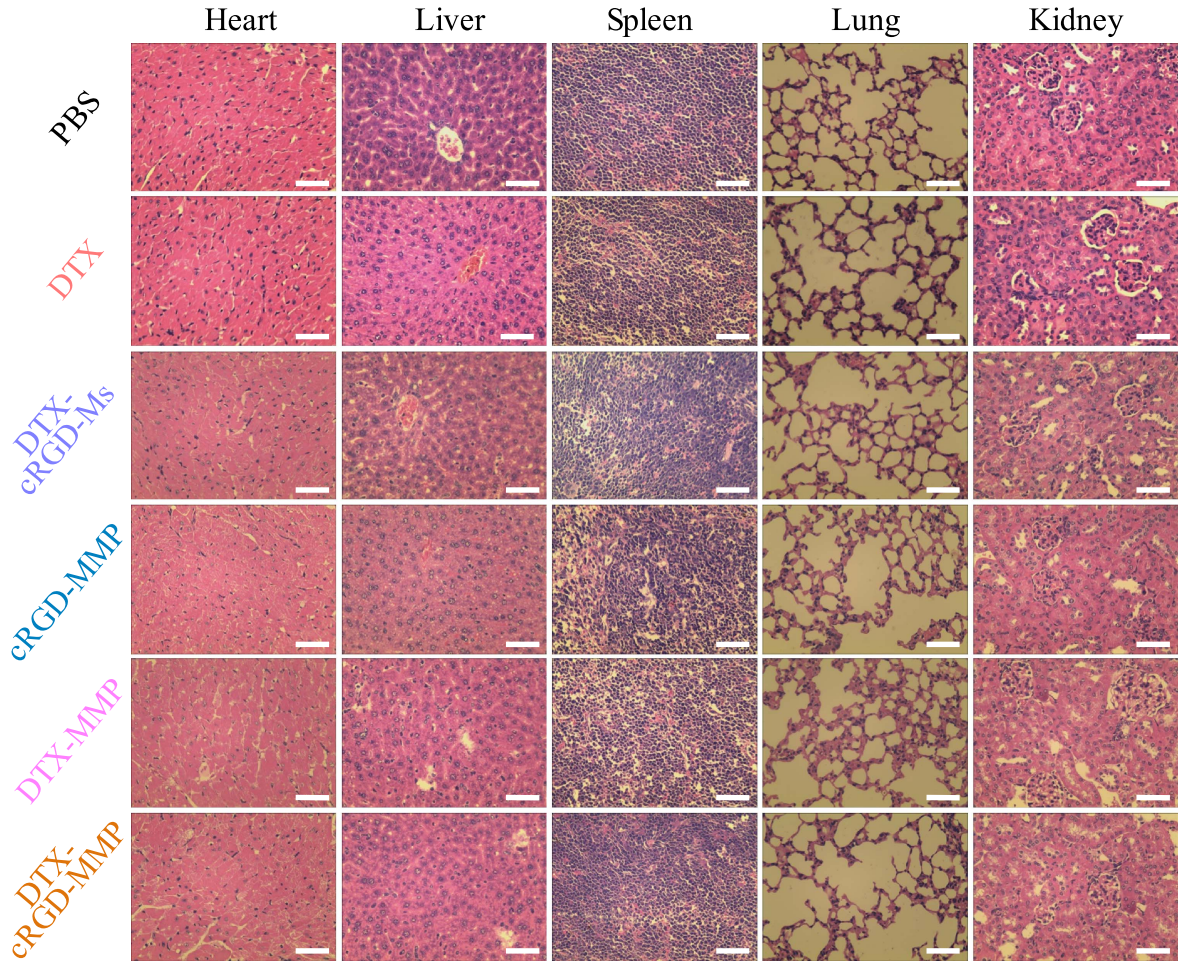

Figure 7. H&E staining assays of the major organs of mice from different treatment groups (DM1 dosage: 1.2 mg kg^{-1}; DTX dosage: 0.7 mg kg^{-1}) (scale bar: 50 μm). The images were acquired using Olympus BX41 microscope at 40× objective.

and DTX. This co-delivery of two mitosis-inhibiting agents appears to be an interesting alternative strategy to reported combinations such as DTX-cisplatin, PTX-DOX, DTX-DOX, and cisplatin-DOX that combine mitosis inhibition and DNA damage [56, 59, 60]. For example, Chen *et al* reported that cRGD-targeting co-delivery of DTX and cisplatin exhibited a remarkable synergistic effect toward B16F10 melanoma with a TIR of 85.1% [56]. Discher *et al* reported that PTX and DOX co-loaded polymersomes had better tolerance and tumor suppression than the free drug cocktail in a subcutaneous MDA-MB-231 human breast cancer model [59]. In line with tumor inhibition results, the DTX-cRGD-MMP group showed a greatly enhanced survival rate with a median survival time of 34 days (figure 6(d)). In comparison, the DTX-cRGD-Ms, cRGD-MMP and free DTX groups revealed shorter median survival times of 21, 26 and 12 days, respectively. The better survival rate of the DTX-cRGD-MMP group as compared to the non-targeting DTX-MMP group signifies the active targeting role of cRGD. No obvious body weight loss was observed for all treatments over the entire experimental period (figure S6), indicating that all formulations are well tolerated by mice. The histological analyses using H&E staining displayed that DTX-cRGD-MMP brought about hardly any damage to the vital organs (figure 7), suggesting that DTX-cRGD-MMP possesses low systemic toxicity. All the above results demonstrate that DTX-cRGD-MMP affords targeted and synergistic treatment of B16F10 melanoma-bearing C57BL/6 mice. DTX-cRGD-MMP with enhanced therapeutic window and reduced systemic toxicity has appeared as a promising nanoplatform for potent cancer chemotherapy.

4. Conclusion

We have developed a docetaxel-encapsulated, cRGD-decorated polymeric micellar mertansine prodrug (DTX-cRGD-MMP) for targeted combinatorial chemotherapy of malignant B16F10 melanoma-bearing C57BL/6 mice. Notably, DTX-cRGD-MMP has a small size, high loading of both DTX and DM1, low drug leakage, and redox-triggered ratiometric release of DM1 and DTX. The *in vitro* studies show that DM1 and DTX in DTX-cRGD-MMP induce a pronounced synergistic antitumor effect in B16F10 cancer cells. DTX-cRGD-MMP exhibits a long circulation time and reaches a remarkably high accumulation of 9.15% ID/g in B16F10 tumor at 12 h post-injection. Interestingly, DTX-cRGD-MMP demonstrates a targeted and strong synergistic treatment of B16F10 melanoma-bearing mice, leading to significantly improved

tumor inhibition and survival rate as compared to the non-targeted control (DTX-MMP) as well as single drug formulations (cRGD-MMP and DTX-cRGD-Ms). It should further be noted that DTX-cRGD-MMP causes little adverse effects. This is a first proof-of-concept study on the combinatorial anticancer effect of DTX and DM1 *in vitro* and *in vivo*. The micellar mertansine prodrug provides a robust nanoplatform for targeted combinatorial chemotherapy.

Acknowledgments

This work was supported by the National Natural Science Foundation of China (NSFC 51373113, 51225302, 51633005) and the Natural Science Foundation of Jiangsu Province (BK20131166).

ORCID

Zhiyuan Zhong https://orcid.org/0000-0003-4175-4741

References

[1] Lehar J *et al* 2009 Synergistic drug combinations tend to improve therapeutically relevant selectivity *Nat. Biotechnol.* **27** 659–66
[2] Von Hoff D D *et al* 2013 Increased survival in pancreatic cancer with nab-paclitaxel plus gemcitabine *N. Engl. J. Med.* **369** 1691–703
[3] He C, Tang Z, Tian H and Chen X 2016 Co-delivery of chemotherapeutics and proteins for synergistic therapy *Adv. Drug. Deliv. Rev.* **98** 64–76
[4] Xu X Y, Ho W, Zhang X Q, Bertrand N and Farokhzad O 2015 Cancer nanomedicine: from targeted delivery to combination therapy *Trends Mol. Med.* **21** 223–32
[5] Narvekar M, Xue H Y, Eoh J Y and Wong H L 2014 Nanocarrier for poorly water-soluble anticancer drugs-barriers of translation and solutions *AAPS PharmaSciTech* **15** 822–33
[6] Mayer L D and Janoff A S 2007 Optimizing combination chemotherapy by controlling drug ratios *Mol. Interv.* **7** 216–23
[7] Schuler M K *et al* 2016 Efficacy and safety of dexrazoxane (DRZ) in sarcoma patients receiving high cumulative doses of anthracycline therapy: a retrospective study including 32 patients *BMC Cancer* **16** 619–27
[8] Ma L, Kohli M and Smith A 2013 Nanoparticles for combination drug therapy *ACS Nano* **7** 9518–25
[9] Jhaveri A, Deshpande P and Torchilin V 2014 Stimuli-sensitive nanopreparations for combination cancer therapy *J. Controlled Release* **190** 352–70
[10] Hu Q, Sun W, Wang C and Gu Z 2016 Recent advances of cocktail chemotherapy by combination drug delivery systems *Adv. Drug. Deliv. Rev.* **98** 19–34
[11] Ke X-Y, Lin N V W, Gao S-J, Tong Y W, Hedrick J L and Yang Y Y 2014 Co-delivery of thioridazine and doxorubicin using polymeric micelles for targeting both cancer cells and cancer stem cells *Biomaterials* **35** 1096–108
[12] Zhang R X, Wong H L, Xue H Y, Eoh J Y and Wu X Y 2016 Nanomedicine of synergistic drug combinations for cancer therapy—strategies and perspectives *J. Controlled Release* **240** 489–503
[13] Zhang Y, Yang C, Wang W, Liu J, Liu Q, Huang F, Chu L, Gao H, Li C and Kong D 2016 Co-delivery of doxorubicin and curcumin by pH-sensitive prodrug nanoparticle for combination therapy of cancer *Sci. Rep.* **6** 21225
[14] Zhang L, Xiao H, Li J, Cheng D and Shuai X 2016 Co-delivery of doxorubicin and arsenite with reduction and pH dual-sensitive vesicle for synergistic cancer therapy *Nanoscale* **8** 12608–17
[15] Xu X, Xie K, Zhang X Q, Pridgen E M, Park G Y, Cui D S, Shi J, Wu J, Kantoff P W and Lippard S J 2013 Enhancing tumor cell response to chemotherapy through nanoparticle-mediated codelivery of siRNA and cisplatin prodrug *Proc. Natl. Acad. Sci. USA* **110** 18638–43
[16] Xiao H H *et al* 2012 A prodrug strategy to deliver cisplatin(IV) and paclitaxel in nanomicelles to improve efficacy and tolerance *Biomaterials* **33** 6507–19
[17] Wei X, Wang Y, Xiong X, Guo X, Zhang L, Zhang X and Zhou S 2016 Codelivery of a π-π stacked dual anticancer drug combination with nanocarriers for overcoming multidrug resistance and tumor metastasis *Adv. Funct. Mater.* **26** 8266–80
[18] Noh I, Kim H O, Choi J, Choi Y, Lee D K, Huh Y M and Haam S 2015 Co-delivery of paclitaxel and gemcitabine via CD44-targeting nanocarriers as a prodrug with synergistic antitumor activity against human biliary cancer *Biomaterials* **53** 763–74
[19] Widdison W C, Wilhelm S D, Cavanagh E E, Whiteman K R, Leece B A, Kovtun Y, Goldmacher V S, Xie H, Steeves R M and Lutz R J 2006 Semisynthetic maytansine analogues for the targeted treatment of cancer *J. Med. Chem.* **49** 4392–408
[20] Cassady J M, Chan K K, Floss H G and Leistner E 2004 Recent developments in the maytansinoid antitumor agents *Chem. Pharm. Bull.* **52** 1–26
[21] Chudasama V, Maruani A and Caddick S 2016 Recent advances in the construction of antibody-drug conjugates *Nat. Chem.* **8** 114–9
[22] Amiri-Kordestani L, Blumenthal G M, Xu Q C, Zhang L, Tang S W, Ha L, Weinberg W C, Chi B, Candau-Chacon R and Hughes P 2014 FDA approval: ado-trastuzumab emtansine for the treatment of patients with HER2-positive metastatic breast cancer *Clin. Cancer Res.* **20** 4436–41
[23] Chari R V, Miller M L and Widdison W C 2014 Antibody–drug conjugates: an emerging concept in cancer therapy *Angew. Chem. Int. Ed.* **53** 3796–827
[24] Sievers E L and Senter P D 2013 Antibody-drug conjugates in cancer therapy *Annu. Rev. Med.* **64** 15–29
[25] Tang X L, Dai H, Zhu Y X, Tian Y, Zhang R B, Mei R B and Li D Q 2014 Maytansine-loaded star-shaped folate-core PLA-TPGS nanoparticles enhancing anticancer activity *Am. J. Transl. Res.* **6** 528–37
[26] Phillips G D L *et al* 2008 Targeting HER2-positive breast cancer with trastuzumab-DM1, an antibody-cytotoxic drug conjugate *Cancer Res.* **68** 9280–90
[27] Zhong P, Meng H, Qiu J, Zhang J, Sun H, Cheng R and Zhong Z 2016 $\alpha_v\beta_3$ Integrin-targeted reduction-sensitive micellar mertansine prodrug: superb drug loading, enhanced stability, and effective inhibition of melanoma growth *in vivo J. Controlled Release* (https://doi.org/10.1016/j.jconrel.2016.12.011)
[28] Varshosaz J, Taymouri S, Hassanzadeh F, Javanmard S H and Rostami M 2014 Self-assembly micelles with lipid core of cholesterol for docetaxel delivery to B16F10 melanoma and HepG2 cells *J. Liposome Res.* **25** 157–65
[29] Yuan J, Liu J L, Song Q, Wang D, Xie W S, Yan H, Zhou J F, Wei Y, Sun X D and Zhao L Y 2016 Photoinduced mild hyperthermia and synergistic chemotherapy by one-pot-synthesized docetaxel-loaded poly(lactic-co-glycolic acid)/

polypyrrole nanocomposites *ACS Appl. Mater. Interfaces* **8** 24445–54
[30] Perol M *et al* 2016 Quality of life results from the phase 3 REVEL randomized clinical trial of ramucirumab-plus-docetaxel versus placebo-plus-docetaxel in advanced/metastatic non-small cell lung cancer patients with progression after platinum-based chemotherapy *Lung Cancer* **93** 95–103
[31] Zhong Y, Meng F, Deng C and Zhong Z 2014 Ligand-directed active tumor-targeting polymeric nanoparticles for cancer chemotherapy *Biomacromolecules* **15** 1955–69
[32] Shi K, Li J, Cao Z, Yang P, Qiu Y, Yang B, Wang Y, Long Y, Liu Y and Zhang Q 2015 A pH-responsive cell-penetrating peptide-modified liposomes with active recognizing of integrin α v β 3 for the treatment of melanoma *J. Controlled Release* **217** 138–50
[33] Guo Y, Niu B, Song Q, Zhao Y, Bao Y, Tan S, Si L and Zhang Z 2016 RGD-decorated redox-responsive d-α-tocopherol polyethylene glycol succinate–poly (lactide) nanoparticles for targeted drug delivery *J. Mater. Chem.* B **4** 2338–50
[34] Poon W, Zhang X, Bekah D, Teodoro J G and Nadeau J L 2015 Targeting B16 tumors *in vivo* with peptide-conjugated gold nanoparticles *Nanotechnology* **26** 285101–11
[35] Han Y C, He Z J, Schulz A, Bronich T K, Jordan R, Luxenhofer R and Kabanov A V 2012 Synergistic combinations of multiple chemotherapeutic agents in high capacity poly(2-oxazoline) micelles *Mol. Pharm.* **9** 2302–13
[36] Liu S, Liu J, Ma Q, Cao L, Fattah R J, Yu Z, Bugge T H, Finkel T and Leppla S H 2016 Solid tumor therapy by selectively targeting stromal endothelial cells *Proc. Natl Acad. Sci. USA* **113** E4079–87
[37] Alibolandi M, Abnous K, Hadizadeh F, Taghdisi S M, Alabdollah F, Mohammadi M, Nassirli H and Ramezani M 2016 Dextran-poly lactide-co-glycolide polymersomes decorated with folate-antennae for targeted delivery of docetaxel to breast adenocarcinoma *in vitro* and *in vivo* *J. Controlled Release* **241** 45–56
[38] Zhang L, Tan L, Chen L, Chen X, Long C, Peng J and Qian Z 2016 A simple method to improve the stability of docetaxel micelles *Sci. Rep.* **6** 36957
[39] Zhang J, Qian Z and Gu Y 2009 *In vivo* anti-tumor efficacy of docetaxel-loaded thermally responsive nanohydrogel *Nanotechnology* **20** 325102–9
[40] Zhong P, Zhang J, Deng C, Cheng R, Meng F and Zhong Z 2016 Glutathione-sensitive hyaluronic acid-SS-mertansine prodrug with a high drug content: facile synthesis and targeted breast tumor therapy *Biomacromolecules* **17** 3602–8
[41] Zhu Y, Wang X, Zhang J, Meng F, Deng C, Cheng R, Jan F and Zhong Z 2017 Exogenous vitamin C boosts the antitumor efficacy of paclitaxel containing reduction-sensitive shell-sheddable micelles *in vivo J. Controlled Release* **250** 9–19
[42] Fang Y, Jiang Y, Zou Y, Meng F, Zhang J, Deng C, Sun H and Zhong Z 2017 Targeted glioma chemotherapy by cyclic RGD peptide-functionalized reversibly core-crosslinked multifunctional poly(ethylene glycol)-b-poly(epsilon-caprolactone) micelles *Acta Biomater.* **50** 396–406
[43] Wayteck L, Dewitte H, De Backer L, Breckpot K, Demeester J, De Smedt S C and Raemdonck K 2016 Hitchhiking nanoparticles: reversible coupling of lipid-based nanoparticles to cytotoxic T lymphocytes *Biomaterials* **77** 243–54
[44] Poon C, He C, Liu D, Lu K and Lin W 2015 Self-assembled nanoscale coordination polymers carrying oxaliplatin and gemcitabine for synergistic combination therapy of pancreatic cancer *J. Controlled Release* **201** 90–9
[45] Rui M, Xin Y, Li R, Ge Y, Feng C and Xu X 2017 Targeted biomimetic nanoparticles for synergistic combination chemotherapy of paclitaxel and doxorubicin *Mol. Pharm.* **14** 107–23
[46] Miao L, Guo S T, Zhang J, Kim W Y and Huang L 2014 Nanoparticles with precise ratiometric co-loading and co-delivery of gemcitabine monophosphate and cisplatin for treatment of bladder cancer *Adv. Funct. Mater.* **24** 6601–11
[47] Liao L, Liu J, Dreaden E C, Morton S W, Shopsowitz K E, Hammond P T and Johnson J A 2014 A convergent synthetic platform for single-nanoparticle combination cancer therapy: ratiometric loading and controlled release of cisplatin, doxorubicin, and camptothecin *J. Am. Chem. Soc.* **136** 5896–9
[48] Luo S, Gu Y, Zhang Y, Guo P, Mukerabigwi J F, Liu M, Lei S, Cao Y, He H and Huang X 2015 Precise ratiometric control of dual drugs through a single macromolecule for combination therapy *Mol. Pharmaceutics* **12** 2318–27
[49] Chin C F, Yap S Q, Li J, Pastorin G and Ang W H 2014 Ratiometric delivery of cisplatin and doxorubicin using tumour-targeting carbon-nanotubes entrapping platinum(IV) prodrugs *Chem. Sci.* **5** 2265–70
[50] Chou T C and Talalay P 1984 Quantitative analysis of dose-effect relationships: the combined effects of multiple drugs or enzyme inhibitors *Adv. Enzyme Regul.* **22** 27–55
[51] Lv S, Tang Z, Li M, Lin J, Song W, Liu H, Huang Y, Zhang Y and Chen X 2014 Co-delivery of doxorubicin and paclitaxel by PEG-polypeptide nanovehicle for the treatment of non-small cell lung cancer *Biomaterials* **35** 6118–29
[52] Cai L, Xu G, Shi C, Guo D, Wang X and Luo J 2015 Telodendrimer nanocarrier for co-delivery of paclitaxel and cisplatin: a synergistic combination nanotherapy for ovarian cancer treatment *Biomaterials* **37** 456–68
[53] Sun H, Meng F, Cheng R, Deng C and Zhong Z 2014 Reduction and pH dual-bioresponsive crosslinked polymersomes for efficient intracellular delivery of proteins and potent induction of cancer cell apoptosis *Acta Biomater.* **10** 2159–68
[54] Lee S-M, O'Halloran T V and Nguyen S T 2010 Polymer-caged nanobins for synergistic cisplatin-doxorubicin combination chemotherapy *J. Am. Chem. Soc.* **132** 17130–8
[55] Kolishetti N, Dhar S, Valencia P M, Lin L Q, Karnik R, Lippard S J, Langer R and Farokhzad O C 2010 Engineering of self-assembled nanoparticle platform for precisely controlled combination drug therapy *Proc. Natl Acad. Sci. USA* **107** 17939–44
[56] Song W, Tang Z, Zhang D, Zhang Y, Yu H, Li M, Lv S, Sun H, Deng M and Chen X 2014 Anti-tumor efficacy of c(RGDfK)-decorated polypeptide-based micelles co-loaded with docetaxel and cisplatin *Biomaterials* **35** 3005–14
[57] Guo S, Lin C M, Xu Z, Miao L, Wang Y and Huang L 2014 Co-delivery of cisplatin and rapamycin for enhanced anticancer therapy through synergistic effects and microenvironment modulation *ACS Nano* **8** 4996–5009
[58] Pradhan R, Ramasamy T, Choi J Y, Kim J H, Poudel B K, Tak J W, Nukolova N, Choi H-G, Yong C S and Kim J O 2015 Hyaluronic acid-decorated poly(lactic-co-glycolic acid) nanoparticles for combined delivery of docetaxel and tanespimycin *Carbohydr. Polym.* **123** 313–23
[59] Ahmed F, Pakunlu R I, Brannan A, Bates F, Minko T and Discher D E 2006 Biodegradable polymersomes loaded with both paclitaxel and doxorubicin permeate and shrink tumors, inducing apoptosis in proportion to accumulated drug *J. Controlled Release* **116** 150–8
[60] Wang H, Zhao Y, Wu Y, Hu Y-l, Nan K, Nie G and Chen H 2011 Enhanced anti-tumor efficacy by co-delivery of doxorubicin and paclitaxel with amphiphilic methoxy PEG-PLGA copolymer nanoparticles *Biomaterials* **32** 8281–90